Influence of Membrane Type on Some Electrical Properties of a Single Microbial Fuel Cell

Hafsa Bouzidi
LMPMP and LEES Laboratories
Faculty of Technology
Ferhat Abbas University
Setif, Algeria
hafsabouzidi@yahoo.fr

Lhadi Otmani
URMES Laboratory
Campus El Maabouda
Ferhat Abbas University
Setif, Algeria
elhadi_otmani@yahoo.fr

Rachida Doufnoune
URMES Laboratory
Campus El Maabouda
Ferhat Abbas University
Setif, Algeria
doufnoune@yahoo.fr

Larbi Zerroual
LMPMP Laboratory
Faculty of Technology
Ferhat Abbas University
Setif, Algeria
zerroual@yahoo.fr

Djafer Benachour
LMPMP Laboratory
Faculty of Technology
Ferhat Abbas University
Setif, Algeria
bendjafer@univ-setif.dz

Received: 8 February 2022 | Revised: 27 February 2022 | Accepted: 14 March 2022

Abstract-The effects of different parameters on the electric output of air-cathode microbial fuel cells were investigated in this work. The single microbial fuel cell was equipped by modifying Proton Exchange Membranes (PEM). Two membrane types were prepared: first by using the combination of Poly Vinyl Alcohol (PVA) with Polystyrene Sulfonate (PSSNa), while the second membrane was elaborated by mixing Poly Vinyl Chloride (PVC) with Methyl Tri-Octyl Ammonium (MTOA) chloride. The PEMs were incorporated into the air-cathode to form a Membrane Electrode Assembly (MEA) to promote electricity generation. PVA/PSSNa and PVC-MTOA membranes were synthesized by solution casting method. Fourier Transform Infrared Spectroscopy (FTIR), Ultraviolet (UV) Visible spectroscopy, Scanning Electronique Microscope (SEM), Differential Scanning Calorimetry (DSC), and water Contact Angle (CA) were used as characterization techniques to explore the membrane structure and properties. The performance and the electric capacity of the microbial fuel cell in real time were operated using an external resistance of 5kΩ. Impedance and resistance capacity were determined using the polarization method. It was found that the internal resistance of the PVA/PSSNa and PVC-MTOA membranes were 50 and 350Ω respectively. The voltage values at open circuit of the cells using PVA/PSSNa and PVC-MTOA membranes were 600mV and 150mV respectively. The values of power, current, and power density, are quite interesting. Cells with PVA/PSSNa and PVC-MTOA membranes gave values of 18.24 and 9.64mW.cm^{-2} respectively.

Keywords-PVA/PSSNa; PVC-MTOA; membrane; single microbial fuel cells; renewable energy; wastewater

I. INTRODUCTION

Human sustainability is determined by deriving factors, among which energy is the most important. During the last decade, fossil fuel commodity has seen a sharp decline because of the harmful effects of fossil fuels on the environment [1]. The problem of pollution pushes the researchers to look for new sources of energy, such as renewable energy [2]. Promising results were acquired by different renewable energy sources, such as solar, wind, tidal, geothermal, and biomass. In the last few years, the research into alternative sources of renewable energy has increased exponentially [3]. However, a new source of energy which is sustainable and environmentally stable was needed [4]. Wastewater treatment is a new energy technology and a bio-energy source [5-6]. The bio-energy process [7] involves the use of microbes to produce electricity. This technology is considered to have tremendous potential [8]. The bacteria available in a bio-convertible substrate were directly used as a catalyst to convert chemical energy to electricity in [9]. It is known that bacteria can generate electricity from organic waste sources [10]. A renewable process was used to generate energy in the form of electricity, in consistent fresh, resourceful manners, through the use of the Microbial Fuel Cells (MFCs) [11]. It was found that in MFCs, energy can be recovered from wastewater treatment, in fact from a wide range of organic compounds present in wastewater [12].

The MFCs consist of two compartments: anodic and cathodic. MFCs are composed of one anodic chamber filled with wastewater and an air cathodic chamber. The anode compartment includes domestic or industrial wastewater with sludge, and the cathode compartment is either used to remove heavy metals or for denitrification [9]. Many MFCs play an important role in producing bio-energy, such as value-added chemicals, via an easy operation, and at low maintenance cost [13]. The removal of organic constituents of wastewater leads

Corresponding author: Djafer Benachour

to the electricity production from the chemical energy stored in chemical bonds [12]. Three mechanisms to generate bioelectricity have been proposed: direct electron transport via membrane bound proteins (e.g. cytochromes), conductive nano-wires, and indirect shuttles via redox mediators (e.g. riboflavin) [14]. With regard to the source abundance, high efficiency, and convenient transportation, the most promising energy conversion devices are Proton Exchange Membranes (PEMs) [15]. PEMs are the most important factor to transport protons, and Nafion membrane has been widely used due to its high conductivity.

Recently, numerous studies have been conducted to find alternative membranes [16]. Desirable PEMs require excellent characteristics, the most important of which is high and stable proton conductivity [17]. An electron flow through the electrodes producing bioelectricity, has been demonstrated experimentally by the bacterial degradation in wastewater [18]. Microbial electricity production offers the possibility of obtaining electrical current from a wide range of soluble or dissolved organic wastes such as artificial, real, and biomass lignocellulosic wastewater [19]. The most important advantages of MFC are wastewater treatment, application of micro-organisms, energy production, and inexpensive biocatalysts [12]. Since the production of electricity in MFCs is related to wastewater treatment, it is considered as one of the most attractive energy sources [20]. MFCs are an emerging technology for simultaneous treatment of wastewater and energy recovery [21], following a similar concept to traditional fuel cells [3]. The process of MFCs was based on the generation of bioelectricity, and this method has been leaded by the bio-potential developed between the bacterial metabolic activity and the electron acceptor conditions, separated by a membrane [22].

The use of MFCs is one potential alternative energy source [3]. The reduction of electron acceptors, with electricity, was harvested in a circuit, by the anode which collected organics oxidized by the electrogenic microorganisms and combined with protons to cathode. The electricity generation and stability of MFCs are radically affected by the microbial communities on the electrode surface [23]. MFC operation includes several steps: first, the carbon dioxide is digested from bacteria and the released electrons are transferred to the anode. Then, electrical energy is generated via the travel of electrons from the anode in an external circuit. Finally, the electrons are taken up by oxygen and hydrogen ions to form water while they are traveling to the cathode to complete the circuit [24]. Recently, a suitable secondary stage process to fully recover the energy embedded in the metabolites and improve treatment efficiency, has been proven using MFC technology [25]. In MFC systems, the produced electrons are not directly transferred from bacteria to their electrons acceptor. The transport process is realized over other factors: cathode, anode, resistance, and membrane which transfer protons to the cathode [26-27]. When the MFCs are operated independently of an electrical device and as an integrated part of an electrical grid that controls the fuel cell output, an external resistance is used to dissipate the electrical energy [20]. The separator is an important factor that affects the design of MFCs [28], which is used to separate anode and cathode. The Cation Exchange Membrane (CEM) and PEM, are investigated as the most important effect in the system: a membrane permits the proton passage and not the substrate, using an organic medium [29-34]. Recently, authors in [9] proposed that the factors which can lower the internal resistance in the MFC, should be optimized to obtain the highest values of voltage density and power.

Most works cited in the literature deal with the use of fuel cells in electrochemical application (batteries), at an industrial scale. In the present work, a new strategy in MFC (single chamber) has been tested using two different PEMs. Combined with a resistance, this separator was based on the order: PVA with PSSNa, and PVC, while the MTOA membrane was synthesized and characterized. The medium contained different organic products and was used as an energy source for the bacteria. Lead dioxide (PbO_2) was used as the cathode material.

II. MATERIALS AND METHODS

PVA with a molecular weight of 130,000 (99% hydrolyzed powder), PSSNa powder with a molecular weight of 70,000, glutaraldehyde (GLA), PVC powder with a molecular weight of 93.92g/mol, MTOA as ionic liquid with a molecular weight of 404.16g/mol, and tetrahydrofuran (THF) with a molecular weight of 72.10g/mol, which was used as a dissolving agent, were all provided by Sigma-Aldrich and were used as such without any further purification. Figure 1 shows the diagram of the experimental procedure.

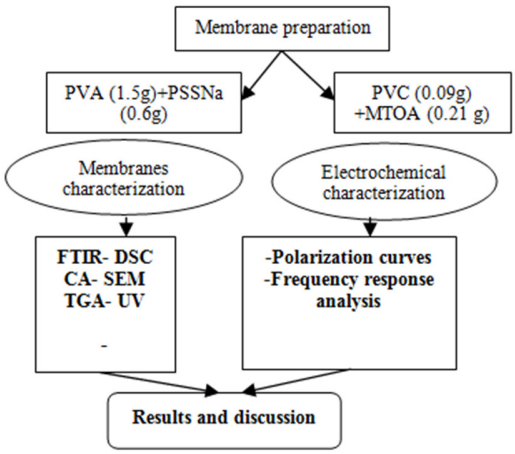

Fig. 1. Experimental diagram.

A. Membrane Preparation

1) PVA-PSSNa Film Preparation

As a first step, 1.5g PVA were dissolved in deionized water and the obtained solution was stirred at 80°C until the PVA particles were completely dissolved. At the same time, the PSSNa solution was prepared by dissolving 0.6g in deionized water. The obtained mixture was further stirred at room temperature until the stabilization of the solution. As a second step, GLA was poured dropwise to the solution and then few drops of HCl solution were added. It is worth noting that a simple pouring of the mixture into a glass sheet with a uniform surface and similar thickness was realized. Finally, the thin film was dried at room temperature for a day.

2) PVC-MTOA Film Preparation

PVC powder (0.09g) and MTOA (0.21g) were dissolved in THF and stirred until complete dissolution. The obtained viscous solution was poured in a plastic mold (diameter = 2.8cm). After the evaporation of the solvent, the thin film was dried at room temperature.

3) Microbial Fuel Cell Configuration and Media Composition

The anodic single chamber is made of glass material with a volume of 250ml (SCHOTT DURAN). The chamber was filled with 200ml of wastewater taken from a water purification station (National Office of Disinfection-Sfiha, Setif, Algeria), with total sprouts, total coliforms, and fecal coliform. The electrode used in this experiment was a carbon fiber fixed in the cap of the chamber. The cathode is made of 0.6g of PbO_2 powder dissolved in 0.5ml ethanol, spread on a piece of stainless steel, left to dry in open air. The Voltage Open Circuit (VOC) was measured with a digital multi-meter. The real time voltage values were recorded with an Arduino program. The carbon fiber rod in the anodic chamber and the cathode were connected into a recorder by the Arduino Uno R3 (open-source electronics prototyping platform, Italy) and the data were registered on a computer. The medium solution was prepared using different components: NH_4Cl (1.50gL^{-1}), KCl (0.1gL^{-1}), Na_2HPO_4 (0.6gL^{-1}), acetate (1.36gL^{-1}), $NaHCO_3$ (2.5gL^{-1}), $CaCl_2$ (0.1gL^{-1}), and yeast extract (0.05gL^{-1}). These components were dissolved in distilled water and the anodic chamber was filled every week.

B. Membrane Characterization

The structure of the thin films was characterized by FTIR spectroscopy, the analysis was recorded on a JASCO-IR spectrometer. The signal scans of 32 were realized in the 4000-400cm^{-1} wavenumber range at a resolution of 4cm^{-1}. UV–visible spectroscopy was used to characterize the structure of the thin films; the scan was carried out using a Shimadzu UV-2401PC UV–visible spectrophotometer in the range of 200–800nm. The optical absorbance of the obtained membranes was recorded and the energy band gap was evaluated from the UV spectrum. The endothermic and exothermic phenomena change of the physical state of the thin films were determined using a diffraction scanning calorimetric (DSC) (Jupiter ,STA 449 F3), the scan was realized in the temperature range of 35-350°C, with a rate of 10°C/min in open air. The variation in weight loss of the membranes as a function of the temperature was examined by TGA analysis, the thermal proprieties were measured using a thermogravimetric analysis (TGA PERKIN-ELMER) apparatus in which the temperature range was set from 25 to 500°C, with a heating rate of 10°C/min. The surface morphology of the membranes was observed by SEM (JEOL, JSM 6510 LV) and the analysis was operated at an acceleration voltage of 30kV. Water CA measurement was used to determine the hydrophilicity or hydrophobicity character of the prepared membranes. This was done using a Ram E-hart CA goniometer/tensiometer. The surface examination was operated at room temperature and with relative humidity of 30 ± 5%. The swelling rate measurements (η) were made through membrane weight, the measurement was based on the calculation of the membrane mass in dry and hydrated state. The swelling rate is expressed as a percentage:

$$\eta = \left[\frac{mf-mi}{mi}\right] * 100 \quad (1)$$

where η is the swelling rate (%), and mf and mi are the final and initial weight of the membrane (g) respectively.

C. MFC Operation and Electrochemical Characterization

The internal resistance of the membranes was measured with the impedance spectroscopy method. The Frequency Response Analysis (FRA) in the beginning and the end (cell discharge) was inspected using a Volta-lab instrument PGSTAT302N, Metrohm Autolab B.V. The frequencies of the operation were oscillated from 1MHz to 0.01Hz with 0.05V amplitude perturbation in 5% of NaCl solution. It should be noted that the different measurement steps of impedance and real time operations were operated in NaCl and bacterial medium solutions respectively. Consequently, the same conditions of MFCs exploited in the impedance measurement were applied. However, Nyquist plot was used to determine the internal resistance of the system after applying the electrochemical impedance spectroscopy technique. Equation (2) gives the relation between the impedance system and the ionic conductivity:

$$\sigma = \frac{L}{R.A} \quad (2)$$

where σ is the ionic conductivity (S/cm^{-1}), L the thickness (cm), A the cross-section area (cm^2) and R the resistance (Ω).

A Nyquist plot was used to determine the internal resistance of the system after applying the electrochemical impedance spectroscopy technique. The membranes were tested in MFCs using wastewater as substrate. A fixed resistance R_{ext} of 5kΩ was used and the result was recorded. A PEM was used in MFCs. The charge-discharge cycle with time gives the voltage as a function of current (current density) (V vs. I), and the power (power density) as a function of current density (P vs. I). The power curve was used to determine the internal resistance. It started at Open Circuit Voltage (OCV), the slope is equal to the internal resistance in the case of a linear polarization curve.

$$E_{cell} = OCV - IR_{int} \quad (3)$$

where E_{cell}, I and R_{int} are the voltage of the cell, current density, and internal resistance respectively.

III. Results and Discussion

A. Spectroscopic Characterization and Morphological Studies

1) FTIR Characterization

PVA-PSSNa was obtained from the reaction of PVA-PSSNa and GLA. The FTIR spectra confirmed the chemical structure. Figure 2 shows the FTIR spectra of PVA-PSSNa. The very wide band that appears at 3356cm^{-1} is related to the stretching vibration of hydroxyl groups of PVA chains. The 2931cm^{-1} band is attributed to alkanes, and ester bands are registered at 1715cm^{-1} and 1435cm^{-1}. The symmetric and asymmetric stretching vibrations due to the sulfonic group are located at 1125cm^{-1} and 1240cm^{-1} respectively. The broad band at 1125cm^{-1} indicates the linking of sulfonic anion with phenyl ring. Additionally, the aromatic functional groups of PSSNa

chain are located at 840cm^{-1}. In the FTIR spectra of PVC-MTOA membrane, the band located at 3673cm^{-1} is associated to a strong free alcohol related to a bond interaction between PVC and MTOA in the presence of the THF as solvent agent. The located bands at 3000-3100cm^{-1} present an amine deformation of the MTOA. A strong alkane C-H band is situated at 2896cm^{-1} related to the PVC. The ammonium groups are located at 2400cm^{-1}. The alkene groups are observed at 2109cm^{-1}, the band recorded at 965cm^{-1} confirmed the existence of the alkene. The appearance of a broad absorption band at 1628cm^{-1} was related to the linked N-H, the bands at 1460cm^{-1} and 1248 cm^{-1} indicated the C-H and C-C bonds respectively, an alcohol group was located at 1378cm^{-1}, and chloroalkane C-Cl was located at 723cm^{-1} [35-36].

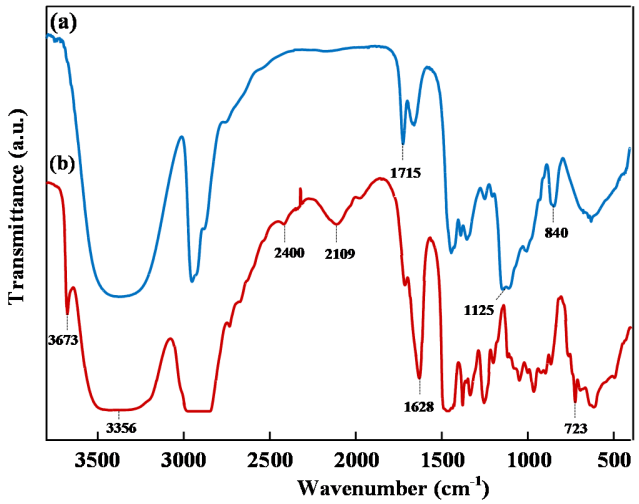

Fig. 2. FTIR spectra of (a) PSSNa/PVA membrane and (b) PVC/MTOA.

2) DSC Characterization

The DSC thermograms are illustrated on Figure 3.

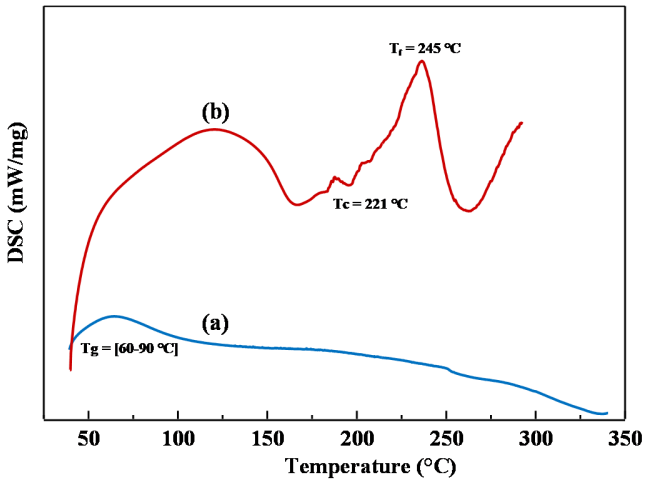

Fig. 3. DSC curve of (a) the blend PVA/PSSNa, (b) the blend PVC/MTOA.

As mentioned above, the mixture was stable and has good miscibility between polymers, thus no visible phase separation between PVA and PSSNa was detected. This confirms the morphology results obtained by SEM. In addition, the thermograms revealed a single glass transition temperature (*Tg*) of the blend in the range of 60 to 90°C, which indicates the total miscibility of the polymers. In the DSC curve obtained on PVC/MTOA membrane, a sudden change in heat transfer at 165.5°C is noticed. This may be explained by the irregularly shaped samples, the ionic liquid being more flexible than the PVC, results in a flexible membrane compared to the PVA/PSSNa membrane. The second endothermic peak at 221°C related to the crystalli-zation temperature (*Tc*) corresponds to the side reaction and decomposition of the membrane while the third peak at 245°C corresponds to the melting point temperature**.** At high temperature all the interactions between the chains are broken.

3) SEM Characterization

SEM images of the membranes are presented in Figure 4. A micrography of the mixture formed by blending PVA, PSSNa, GLA, is also reported in the same Figure.

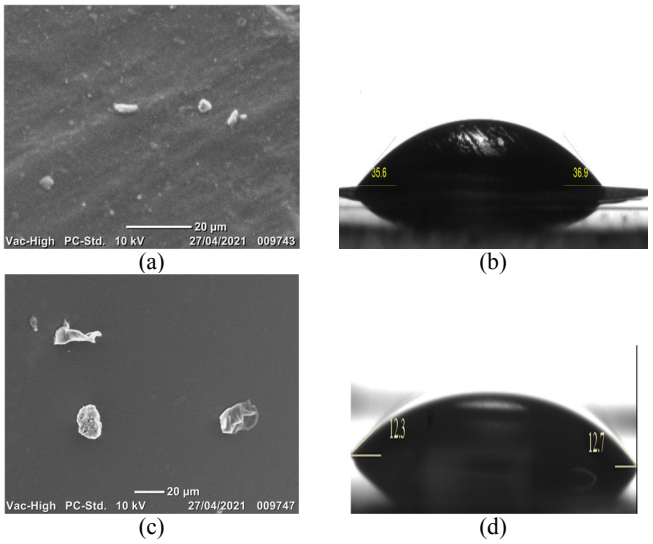

Fig. 4. (a) SEM of the PVA/PSSNa, (b) water CA of PVA/PSSNa, (c) SEM of the PVC/MTOA, and (d) water CA of PVC/MTOA.

As can be seen in Figure 4, no phase separation was observed for the prepared membranes. The PVA/PSSNa presents a good combination between the two polymers and homogenous surface. PVC/MTOA membrane exhibits a smooth and homogeneous nonporous surface too. The obtained membranes are transparent and have good clarity, implying good compatibility between the ionic liquid and the polymer. This leads to more contact area and more compatibility to form a bio-film (in which the ionic charge is produced because it is formed with the bacteria found in the medium).

4) Contact Angle and Swelling Rate Characterization

The hydrophilicity of the membranes was evaluated using the water CA technique. It can be noted that for PVA/PSSNa membrane the values varied from 35.6° to 36.9°, while for PVC/MTOA membrane, the contact angle values varied from 12.3° to 12.7°. The polymers containing sulfonic acid groups

transport protons via the vehicular mechanism, relying on the presence of water PVA/PSSNa membrane. The water adsorption of the PVC/MTOA membrane is attributed to the ionic liquid group. Table I summarizes the CA and the swelling rate values of PVA/PSSNa and PVC/MTOA membranes, it confirms the results observed in Figure 4.

TABLE I. CONTACT ANGLE AND SWELLING RATE VALUES OF PVA/PSSNa AND PVC/MTOA MEMBRANES

Membrane	Contact angle (°)	Swelling rate (%)
PVA/PSSNa	35.6-36.9	78.38
PVC/MTOA	12.3-12.7	86.07

The water absorption of the two membranes was studied by immersing the membranes in deionized solution. The weight of the membranes was measured before and after immersion. The membranes show that the water uptake was elevated due to water molecule mobility. The elevated water-uptake improves the swelling rate of PVA/PSSNA (η = 78%) and PVC/MTOA (η = 86%) membranes. The problem encountered is that the membranes never return to their initial states after being immersed in water. Consequently, the membranes have a good water uptake, and this will increase the proton conductivity.

5) TGA Characterization

The thermal stability of PVA/PSSNa and PVC/MTOA membranes under nitrogen atmosphere, was evaluated by thermogravimetric analysis. The TGA thermograms are presented in Figure 5.

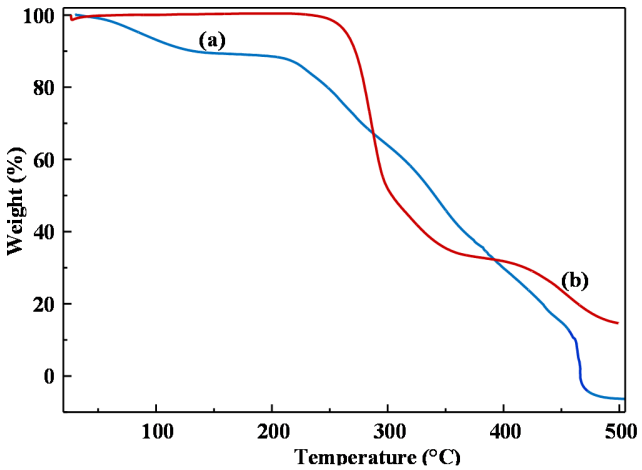

Fig. 5. TGA curves of (a) the blend PVA/PSSNa, (b) the blend PVC/MTOA.

The thermogram shows a typical three-step degradation of PVA/PSSNa. A small weight loss was observed at about 61°C due to the evaporation of physisorbed water. The second weight loss, which occurred between 217 and 462°C, corresponds to the degradation of PVA/PSSNa. The third weight loss, above 465°C, was due to the decomposition of the backbones of the materials. The curves showed a typical two-step degradation pattern of the PVC/MTOA membrane. No obvious weight loss was observed until 250°C. The weight loss recorded between 253 and 415°C corresponds to the degradation of PVC, whereas the second weight loss in the range 415-495°C is due to the decomposition of MTOA.

6) UV Characterization

The UV spectra of PVA/PSSNa and PVC/MTOA are presented in Figure 6. The main peaks are located at 227-193.5nm and are attributed to PVA/PSSNa and PVC/MTOA respectively, which indicates a significant interaction between polymers, while no phase separation was noticed.

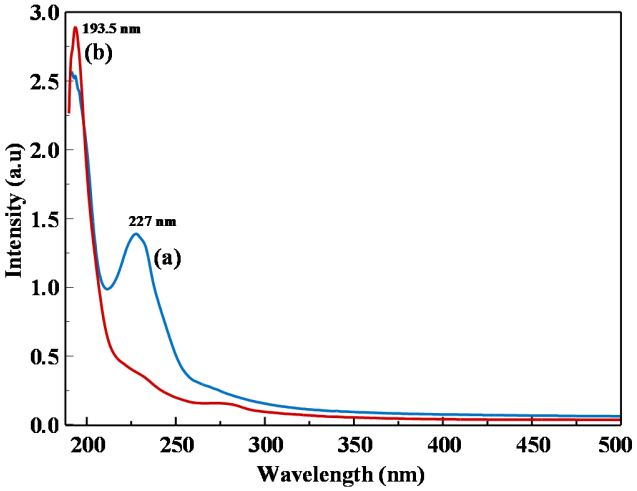

Fig. 6. UV visible spectra of (a) PSSNa/PVA and (b) PVC/MTOA membranes.

B. Electrochemical Monitoring

Figure 7 shows the Nyquist plots for the supported membranes, based on PVA/PSSNa and PVC/MTOA. The values of the internal resistance and the ionic conductivity are given in Table II. The internal resistance values are 54.12 and 350Ω for PVA/PSSNa and PVC/MTOA respectively. These values confirm the high conductivity of PVA/PSSNa membrane.

TABLE II. MAIN CHARACTERISTICS OF THE MEMBRANES

Membrane	Thickness (µm)	Area (cm^2)	Internal resistance (Ω)	Ionic conductivity ($S\ cm^{-1}$)
PVA/PSSNa	301	0.785	54.12	$1.02*10^{-4}$
PVC/MTOA	230	0.785	350	$8.37*10^{-6}$

After the discharge of the cells, it was noticed that the internal resistance was approximately 62Ω for the PVA/PSSNa membrane. Almost no difference in the internal resistance value before and after the test was detected, while in the case of PVC/MTOA membrane, the internal resistance significantly increased at the end of the test (1200Ω). This difference can be related to the membrane aging. The ionic conductivities of the PVA/PSSNa and PVC/MTOA membranes are respectively 1.02×10^{-4} and 8.37×10^{-6}S/cm. PVA/PSSNa presents higher proton conductivity compared to PVC/MTOA (see Table II).

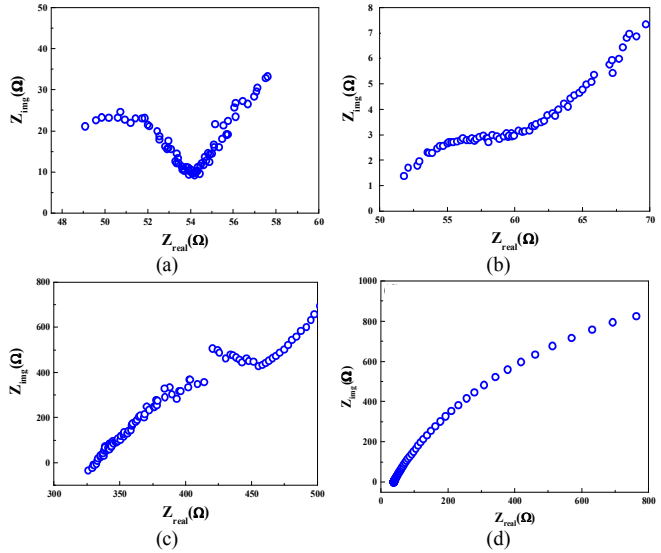

Fig. 7. Frequency response analysis of membranes based on (a,c) PVA/PSSNa and (b,d) PVC/MTOA membranes.

TABLE III. ELECTRICAL PARAMETERS OF THE MEMBRANES

	External resistance (kΩ)	Time (weeks)	OCV (mV)	Maximum power (mW.cm^{-2})	Maximum voltage (mV)	Maximum current density (mA.cm^{-2})
PVA/ PSSNa	5	1	604	18.24	386.02	0.14
		2	377	9.05	278.49	0.09
		3	341	6.25	239.78	0.09
		4	342	6.98	239.78	0.09
		5	300	4.98	205.38	0.08
PVC/ MTOA	5	1	156	1.50	422.58	0.04
		2	156	1.55	450.54	0.04
		3	198	2.50	212.9	0.05
		4	389	9.64	212.9	0.10
		5	292	5.26	119.75	0.07

High electron transfer from the anodic chamber to the cathode leads to high current. The anode potential should be low and the cathode potential should be high in order to have a maximum fuel cell performance. The metabolic activities of the biocatalyst and the respective energy dissipation can affect the anode potential. In a biofuel cell, bacteria drain off their electrons to the anode.

Figure 8 shows the polarization curve of MFCs filled with wastewater. The two curves describe the voltage and power as functions of the current density to identify the maximum output power density of MFCs. The obtained open circuit voltage was 604mV for the PVA/PSSNa and 156mV for PVC/MTOA (Table III). Figure 9 shows the polarization curve of MFCs filled with medium. The power and the current density increased after four weeks in the case of the PVC/MTOA membrane but the voltage decreased from the first week. The maximal values were obtained in the second week of using the medium and were 9.64mw/cm^2 power and 0.10mA/cm^2 current density.

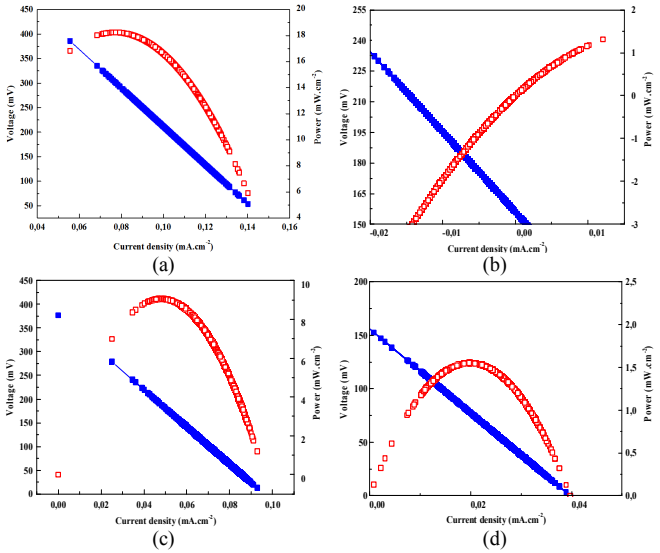

Fig. 8. Polarization curves of the MFC using different membranes (in wastewater).

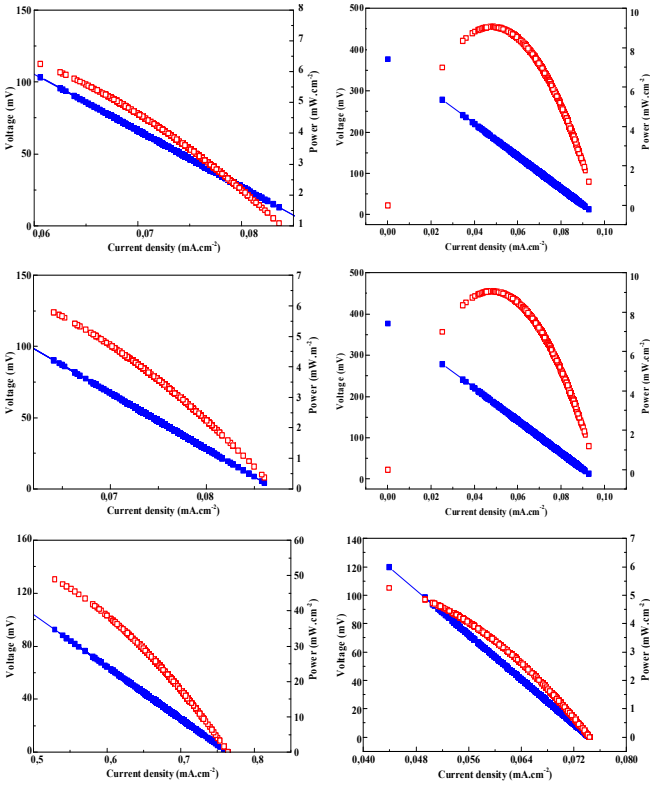

Fig. 9. Polarization curves of the MFC using different membranes (using the medium).

Regarding the PVA/PSSNa membrane, the maximal values were observed during the first week and they were about 18.24mw/cm^2 power and 0.14mA/cm^2 current density. The cell decreased after that and this decrease of power generation can be related to the structure and to the effect of the internal resistance of the two membranes: the PVC/MTOA membrane is more flexible (from the mechanical point of view) and more

resistant (from the electrical point of view) than the PVA/PSSNa membrane. This difference will impact the bio-film formed, while the PVA/PSSNa will be more effective in the electricity generation. Accordingly, the electron transfer from the anodic chamber to the cathode decreases according to the bio-film forming the electrical resistances of the electrodes, the membrane internal resistance and electrolyte, the power drops due to the increasing Ohmic losses, and the electrode overpotentials to the point where no more power is produced. [37-39].

In a previous similar work [21], the authors used a PVC-based membrane, however the conductivity obtained was not as good as the one obtained in this study for the PVC/MTOA membrane. In addition, we used the CA parameter to evaluate the membrane surface capacity for matter adsorption, which, to the best of our knowledge, is reported for the first time.

IV. CONCLUSION

In this paper, MFCs were used to directly generate electricity from the oxidation of dissolved organic matter. However, the optimization of MFCs requires more knowledge about the factors that can increase the power output such as the capacity of proton exchange system which can affect the system characteristics, particularly the internal resistance and the external resistance. The power (P) was calculated according to $P = IV$ ($I = V/R$), where I (A) is the current, V (V) is the voltage, and R (Ω) is the resistance. The prepared assisted cross-linked PVA-PSSNa membrane has a good ionic conductivity and a good miscibility and thermal stability. In addition, it exhibits high proton exchange capacity and lower internal resistance, compared to the PVC/MTOA membrane which has a high internal resistance and a long term to discharge. It has also good miscibility, a hydrophilic character, and a good thermal stability.

AUTHORSHIP CONTRIBUTION STATEMENT

The results presented here are part of a Ph.D. thesis work. H. Bouzidi, as a Ph.D. student, conducted most of the experimental and characterization work. L. Otmani and R. Doufnoune prepared and provided the PVA-PSSNa membrane, L. Zerroual (thesis co-advisor) helped in the electrochemical experimental work, while D. Benachour (thesis advisor) did the editing.

REFERENCES

[1] E. Ogungbemi *et al.*, "Fuel cell membranes – Pros and cons," *Energy*, vol. 172, pp. 155–172, Apr. 2019, https://doi.org/10.1016/j.energy.2019.01.034.

[2] J. Liu, "China's renewable energy law and policy: A critical review," *Renewable and Sustainable Energy Reviews*, vol. 99, pp. 212–219, Jan. 2019, https://doi.org/10.1016/j.rser.2018.10.007.

[3] A. J. Slate, K. A. Whitehead, D. A. C. Brownson, and C. E. Banks, "Microbial fuel cells: An overview of current technology," *Renewable and Sustainable Energy Reviews*, vol. 101, pp. 60–81, Mar. 2019, https://doi.org/10.1016/j.rser.2018.09.044.

[4] J. Chouler *et al.*, "Towards effective small scale microbial fuel cells for energy generation from urine," *Electrochimica Acta*, vol. 192, pp. 89–98, Feb. 2016, https://doi.org/10.1016/j.electacta.2016.01.112.

[5] D. J. Batstone, T. Hulsen, C. M. Mehta, and J. Keller, "Platforms for energy and nutrient recovery from domestic wastewater: A review," *Chemosphere*, vol. 140, pp. 2–11, Dec. 2015, https://doi.org/10.1016/j.chemosphere.2014.10.021.

[6] H.-L. Song, Y. Zhu, and J. Li, "Electron transfer mechanisms, characteristics and applications of biological cathode microbial fuel cells – A mini review," *Arabian Journal of Chemistry*, vol. 12, no. 8, pp. 2236–2243, Dec. 2019, https://doi.org/10.1016/j.arabjc.2015.01.008.

[7] Z. Zhang, R. Miyajima, T. Inada, D. Miyagi, and M. Tsuda, "Novel energy management method for suppressing fuel cell degradation in hydrogen and electric hybrid energy storage systems compensating renewable energy fluctuations," *International Journal of Hydrogen Energy*, vol. 43, no. 14, pp. 6879–6886, Apr. 2018, https://doi.org/10.1016/j.ijhydene.2018.02.124.

[8] D. Lal, "Microbes to Generate Electricity," *Indian Journal of Microbiology*, vol. 53, no. 1, pp. 120–122, Mar. 2013, https://doi.org/10.1007/s12088-012-0343-2.

[9] T. H. Choi *et al.*, "Electrochemical performance of microbial fuel cells based on disulfonated poly(arylene ether sulfone) membranes," *Journal of Power Sources*, vol. 220, pp. 269–279, Dec. 2012, https://doi.org/10.1016/j.jpowsour.2012.07.109.

[10] B. E. Logan and J. M. Regan, "Electricity-producing bacterial communities in microbial fuel cells," *Trends in Microbiology*, vol. 14, no. 12, pp. 512–518, Dec. 2006, https://doi.org/10.1016/j.tim.2006.10.003.

[11] K. Senthilkumar and M. Naveen Kumar, "Generation of bioenergy from industrial waste using microbial fuel cell technology for the sustainable future," in *Refining Biomass Residues for Sustainable Energy and Bioproducts*, R. P. Kumar, E. Gnansounou, J. K. Raman, and G. Baskar, Eds. Cambridge, MA, United States: Academic Press, 2020, pp. 183–193.

[12] R. Tajdid Khajeh, S. Aber, and K. Nofouzi, "Efficient improvement of microbial fuel cell performance by the modification of graphite cathode via electrophoretic deposition of CuO/ZnO," *Materials Chemistry and Physics*, vol. 240, Jan. 2020, Art. no 122208, https://doi.org/10.1016/j.matchemphys.2019.122208.

[13] Y. Li, C. Cheng, S. Bai, L. Jing, Z. Zhao, and L. Liu, "The performance of Pd-rGO electro-deposited PVDF/carbon fiber cloth composite membrane in MBR/MFC coupled system," *Chemical Engineering Journal*, vol. 365, pp. 317–324, Jun. 2019, https://doi.org/10.1016/j.cej.2019.02.048.

[14] S.-H. Chang *et al.*, "Feasibility study of surface-modified carbon cloth electrodes using atmospheric pressure plasma jets for microbial fuel cells," *Journal of Power Sources*, vol. 336, pp. 99–106, Dec. 2016, https://doi.org/10.1016/j.jpowsour.2016.10.058.

[15] Q. Zhao *et al.*, "Effect of aminated nanocrystal cellulose on proton conductivity and dimensional stability of proton exchange membranes," *Applied Surface Science*, vol. 466, pp. 691–702, Feb. 2019, https://doi.org/10.1016/j.apsusc.2018.10.063.

[16] B. Lin *et al.*, "Protic ionic liquid/functionalized graphene oxide hybrid membranes for high temperature proton exchange membrane fuel cell applications," *Applied Surface Science*, vol. 455, pp. 295–301, Oct. 2018, https://doi.org/10.1016/j.apsusc.2018.05.205.

[17] H. Gao *et al.*, "Improving the proton conductivity of proton exchange membranes via incorporation of HPW-functionalized mesoporous silica nanospheres into SPEEK," *International Journal of Hydrogen Energy*, vol. 43, no. 48, pp. 21940–21948, Nov. 2018, https://doi.org/10.1016/j.ijhydene.2018.08.214.

[18] K. Tota-Maharaj and P. Paul, "Performance of pilot-scale microbial fuel cells treating wastewater with associated bioenergy production in the Caribbean context," *International Journal of Energy and Environmental Engineering*, vol. 6, no. 3, pp. 213–220, Sep. 2015, https://doi.org/10.1007/s40095-015-0169-x.

[19] R. Huarachi-Olivera *et al.*, "Bioelectrogenesis with microbial fuel cells (MFCs) using the microalga Chlorella vulgaris and bacterial communities," *Electronic Journal of Biotechnology*, vol. 31, pp. 34–43, Jan. 2018, https://doi.org/10.1016/j.ejbt.2017.10.013.

[20] A. Gonzalez del Campo, P. Canizares, J. Lobato, M. Rodrigo, and F. J. Fernandez Morales, "Effects of External Resistance on Microbial Fuel Cell's Performance," in *Environment, Energy and Climate Change II: Energies from New Resources and the Climate Change*, G. Lefebvre, E.

Jimenez, and B. Cabanas, Eds. New York, NY, USA: Springer, 2016, pp. 175–197.

[21] M. J. Salar-Garcia, V. M. Ortiz-Martinez, A. P. de los Rios, and F. J. Hernandez-Fernandez, "A method based on impedance spectroscopy for predicting the behavior of novel ionic liquid-polymer inclusion membranes in microbial fuel cells," *Energy*, vol. 89, pp. 648–654, Sep. 2015, https://doi.org/10.1016/j.energy.2015.05.149.

[22] M. Rahimnejad, T. Jafary, F. Haghparast, G. Najafpour, and A. A. Ghoreyshi, "Nafion as a nanoproton conductor in microbial fuel cells," *Turkish Journal of Engineering and Environmental Sciences*, vol. 34, no. 4, pp. 289–292, Feb. 2011, https://doi.org/10.3906/muh-1006-48.

[23] S. Xin *et al.*, "Electricity generation and microbial community of single-chamber microbial fuel cells in response to Cu2O nanoparticles/reduced graphene oxide as cathode catalyst," *Chemical Engineering Journal*, vol. 380, Jan. 2020, Art. no. 122446, https://doi.org/10.1016/j.cej.2019.122446.

[24] N. S. N. Hisham *et al.*, "Microbial fuel cells using different types of wastewater for electricity generation and simultaneously removed pollutant," *Journal of Engineering Science and Technology*, vol. 8, no. 3, pp. 316–325, 2013.

[25] J. L. Varanasi, S. Roy, S. Pandit, and D. Das, "Improvement of energy recovery from cellobiose by thermophillic dark fermentative hydrogen production followed by microbial fuel cell," *International Journal of Hydrogen Energy*, vol. 40, no. 26, pp. 8311–8321, Jul. 2015, https://doi.org/10.1016/j.ijhydene.2015.04.124.

[26] J. Grandgirard, D. Poinsot, L. Krespi, J.-P. Nenon, and A.-M. Cortesero, "Costs of secondary parasitism in the facultative hyperparasitoid Pachycrepoideus dubius: does host size matter?," *Entomologia Experimentalis et Applicata*, vol. 103, no. 3, pp. 239–248, 2002, https://doi.org/10.1046/j.1570-7458.2002.00982.x.

[27] C.-Y. Chen, T.-Y. Chen, and Y.-C. Chung, "A comparison of bioelectricity in microbial fuel cells with aerobic and anaerobic anodes," *Environmental Technology*, vol. 35, no. 3, pp. 286–293, Feb. 2014, https://doi.org/10.1080/09593330.2013.826254.

[28] X. Zhang, S. Cheng, X. Wang, X. Huang, and B. E. Logan, "Separator Characteristics for Increasing Performance of Microbial Fuel Cells," *Environmental Science & Technology*, vol. 43, no. 21, pp. 8456–8461, Nov. 2009, https://doi.org/10.1021/es901631p.

[29] B. E. Logan *et al.*, "Microbial Fuel Cells: Methodology and Technology," *Environmental Science & Technology*, vol. 40, no. 17, pp. 5181–5192, Sep. 2006, https://doi.org/10.1021/es0605016.

[30] B. Zhang and J. Ni, "Enhancement of Electricity Generation and Sulfide Removal in Microbial Fuel Cells with Lead Dioxide Catalyzed Cathode," in *4th International Conference on Bioinformatics and Biomedical Engineering*, Chengdu, China, Jun. 2010, pp. 1–4, https://doi.org/10.1109/ICBBE.2010.5514899.

[31] A. S. Alghamdi, "Synthesis and Mechanical Characterization of High Density Polyethylene/Graphene Nanocomposites," *Engineering, Technology & Applied Science Research*, vol. 8, no. 2, pp. 2814–2817, Apr. 2018, https://doi.org/10.48084/etasr.1961.

[32] S. Chaoui, D. Smail, A. Hellati, and D. Benachour, "Effect of Starch Nanocrystals on the Properties of Low Density Polyethylene/Thermoplastic Starch Blends," *Engineering, Technology & Applied Science Research*, vol. 10, no. 4, pp. 5875–5881, Aug. 2020, https://doi.org/10.48084/etasr.3608.

[33] N. el H. Belkham, D. Benachour, and A. Mehamha, "Elaboration and Physico-Chemical Characterization of the Gibbsite Li(OH)3 Hybrid Material," *Engineering, Technology & Applied Science Research*, vol. 11, no. 1, pp. 6740–6744, Feb. 2021, https://doi.org/10.48084/etasr.3988.

[34] A. S. Alghamdi, "Creep Resistance of Polyethylene-based Nanocomposites," *Engineering, Technology & Applied Science Research*, vol. 9, no. 4, pp. 4367–4370, Aug. 2019, https://doi.org/10.48084/etasr.2759.

[35] R. M. Silverstein, G. C. Bassler, and C. T. Morrill, *Spectrometric identification of organic compounds*, 3d ed. New York, NY, USA: Wiley, 1974.

[36] S. Chaibi, D. Benachour, M. Merbah, M. Esperanza Cagiao, and F. J. Balta Calleja, "The role of crosslinking on the physical properties of gelatin based films," *Colloid and Polymer Science*, vol. 293, no. 10, pp. 2741–2752, Oct. 2015, https://doi.org/10.1007/s00396-015-3660-2.

[37] D. Chalal, R. Garuz, D. Benachour, J. Boucle, and B. Ratier, "Influence of an electrode self-protective architecture on the stability of inverted polymer solar cells based on P3HT:PCBM with an active area of 2cm2," *Synthetic Metals*, vol. 212, pp. 161–166, Feb. 2016, https://doi.org/10.1016/j.synthmet.2015.12.021.

[38] H. Satha, I. Kouadri, and D. Benachour, "Thermal, Structural and Morphological Studies of Cellulose and Cellulose Nanofibers Extracted from Bitter Watermelon of the Cucurbitaceae Family," *Journal of Polymers and the Environment*, vol. 28, no. 7, pp. 1914–1920, Jul. 2020, https://doi.org/10.1007/s10924-020-01735-6.

[39] M. Hafani, M. A. Chemrak, M. Djennad, and D. Benachour, "Formulation and characterization of a new PET-based membrane for methane gas dehydration," *Polymer-Plastics Technology and Materials*, vol. 60, no. 15, pp. 1605–1619, Oct. 2021, https://doi.org/10.1080/25740881.2021.1912091.